

A Compact Novel Fractal Based Rectenna for RF Energy Harvesting

Nipa Panchal Biswas¹, Puja Das^{1,*}, Anirban Karmakar¹, and Tamasi Moyra Panua²

¹Department of Electronics and Communication Engineering (ECE), Tripura University (A Central University), India

²Department of Electronics and Communication Engineering (ECE), National Institute of Technology, Agartala, Tripura, India

ABSTRACT: With the advancement of wireless communication, Radio Frequency (RF) energy harvesting has gained significant attention over the past decade. RF energy harvesting is emerging as a sustainable alternative to conventional batteries, enabling self-powered operation in wireless sensor networks and Internet-of-Things (IoT) devices. This work presents a single band fractal based rectenna (Antenna with Rectifier) system for efficient RF energy harvesting. Here, a single-diode shunt rectifier converts RF signals into usable DC power which will be usable to many self-powered wireless devices applications. The results show that the proposed antenna ($41.03 \times 37.24 \times 1.6$ mm³) features a bandwidth of 45.64% ranging from 2.08 GHz to 3.31 GHz and reflection coefficient of -60 dB at 2.45 GHz. The proposed antenna obtained maximum gain of 6.02 dBi with maximum radiation efficiency of 71.4% at 2.45 GHz. A diode rectifier with single stub matching network is used in which a HSMS2860 Schottky diode is connected in shunt for the rectification. The proposed rectifier obtains PCE of 70.07% and DC output voltage of 1.664 V at 5 dBm input power (P_{in}).

1. INTRODUCTION

Radio Frequency Energy Harvesting (RFEH) is a technology that captures ambient RF signals from sources like Wi-Fi routers, cellular towers, and broadcasting stations, and converts them into usable electrical energy. A typical RFEH system consists of a receiving antenna, a rectifier circuit (often integrated into a rectenna), and a power management unit. The antenna collects RF signals, which are converted from AC-to-DC by the rectifier, and then regulated and stored by the power management circuit to power low-energy devices such as IoT sensors, medical implants, and wireless nodes. This approach reduces dependence on batteries, lowers maintenance costs, and utilizes existing RF emissions, making it ideal for remote or hard-to-reach applications. The rectenna is a critical component, designed for high RF-to-DC conversion. It is the energy used to power the electronic gadget [1]. It consists of a rectifier, matching network, and receiving antenna. The function of the rectifier is to convert RF Power to DC power [2]. The rectifier usually contains a combination of one or more Schottky diodes in series or shunt. In rectenna design, antenna is used to capture the ambient RF energy, and rectifier is used to convert harvested power signals into DC power. The rectenna converts and harvests the radio frequency signals from broadcast stations, radio towers, and Wi-Fi routers [3, 4]. The rectenna's performance depends upon the rectifier. Several methods, such as etching slots on the antenna or incorporating fractal geometry into the design of the antenna, have been investigated in order to create a compact-sized antenna [5–8]. These methods are currently a well-liked and suitable option.

A fractal is an object with fractional dimensions that is produced recursively using self-similar structures. Benoit Mandelbrot explained it as being derived from the Latin word “frac-

tus”, which means shattered or fractured [9]. The two primary characteristics of fractal antennas are self-similarity and space-filling [10]. The antenna's size is decreased, and its electrical length is increased in a compact physical space because of the space filling property [12]. The self-similarity property suggests that an antenna patch is divided into smaller fragments, each of which is the smallest segment or smaller size of the main antenna [11]. Fractal antennas are increasingly employed in RF energy harvesting systems due to their compact form factor, high radiation efficiency, self-repeating, and space-filling geometries which enable operation over a wide range of frequency bands simultaneously, including Global System for Mobile Communication (GSM), Wi-Fi, Long-Term Evolution (LTE), and Industrial, Scientific, and Medical band (ISM) bands. Additionally, fractal antennas can be engineered to support either directional or omnidirectional radiation patterns depending on application requirements. Omnidirectional designs are particularly advantageous in dynamic or non-line-of-sight environments, as they facilitate energy collection from multiple incident directions, enhancing the spatial diversity and consistency of harvested power. This work presents a single-band microstrip fractal antenna for RF energy harvesting for 2.45 GHz to be used for Wi-Fi/LTE band, Bluetooth, RFID, wireless cameras and drones. 2.45 GHz lies in the ISM band (Industrial, Scientific, and Medical band) which are license-free worldwide. The reason for choosing the 2.45 GHz frequency is that it offers a perfect balance among range, speed, antenna size, and safe heating properties, making it the most versatile ISM frequency in the world. It can be used in wireless communication, radar, and sensing, scientific or medical field. The proposed design features a single-diode rectifier with an impedance matching network to optimize RF-to-DC conversion efficiency. Section 2 details the antenna geometry, while Section 3 presents simulated performance analyses. Section 4

* Corresponding author: Puja Das (pujadas199628@gmail.com).

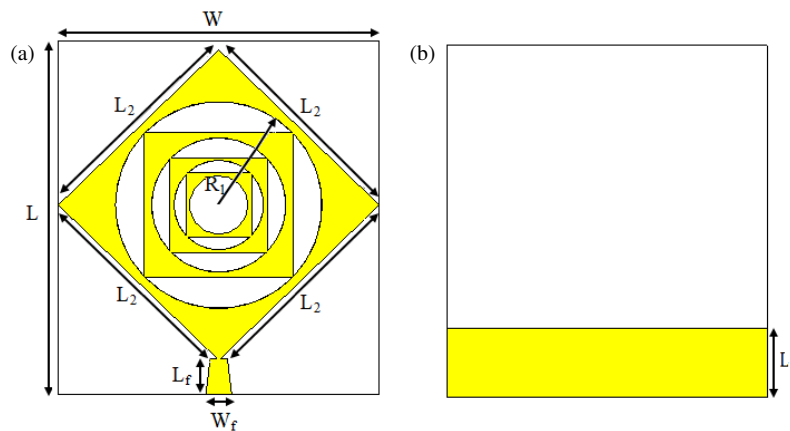


FIGURE 1. Schematic layout of the proposed antenna. (a) Front view. (b) Back view.

covers experimental validation, and Section 5 describes the rectifier configuration. Section 6 explains the experimental validation of the rectenna system, and Section 7 concludes with key findings.

2. GEOMETRICAL DESCRIPTION OF THE PROPOSED ANTENNA

Front view and back view of the proposed fractal antenna are shown in Figures 1(a) and (b). The antenna design employs the fractal geometry, realized by etching iterative fractal slots onto a square microstrip radiating patch. The antenna is fabricated on a lossy FR-4 dielectric substrate characterized by a relative permittivity of 4.3, loss tangent of 0.02, and thickness of 1.6 mm. The square radiating patch measures 25.90×25.90 mm 2 patterned on the substrate's top layer, while the substrate itself measures 41.03×37.24 mm 2 . A partial ground plane with a length (L_1) of 8 mm is implemented on the substrate's bottom layer. The electromagnetic behaviour, particularly the reflection coefficient (S_{11}), is strongly influenced by the geometric parameters of the patch, substrate, and ground plane. The antenna is excited via a 50Ω microstrip feed line with a width (W_f) of 2 mm and length (L_f) of 4.20 mm. The fractal geometry introduces a fractal slot with an outer radius of 12 mm. To enhance impedance bandwidth, a tapered microstrip feed line is incorporated, providing a smooth transition between the feed line and fractal patch. The fundamental resonant frequency at approximately 2.45 GHz is tuned by adjusting the effective electrical length (L_{eff}) of the fractal structure, as expressed by the fractal length relation in Equation (1).

$$L_{eff} = L_0 \times S^n \quad (1)$$

where:

L_0 = initial side length of the largest square (first iteration)

S = scaling factor of the fractal (depends on how the geometry is reduced at each stage, and it is 1/3 for square fractal)

n = number of fractal iterations

L_{eff} = effective length of square fractal

The resonant frequency of 2.45 GHz for this proposed antenna is calculated by this formula as given in Equation (2):

$$F_r = \frac{c}{2 \times L_{eff}} \quad (2)$$

where,

$c = 3 \times 10^8$ m/sec is the speed of the light

F_r = Resonant frequency of the proposed antenna

Figure 2 shows the step by step design procedure for easier understanding of the whole design process of the proposed antenna. The proposed antenna design undergoes a step-by-step evolution to achieve optimal performance at the 2.45 GHz band. The design progression involves structural modifications to both the radiating element and feeding mechanism to improve key performance metrics such as resonant frequency alignment, return loss (S_{11}), and bandwidth. In Antenna 1, a conventional square microstrip patch antenna is designed and fed using a front-side tapered microstrip feed line. The tapered feed is employed to provide a gradual impedance transition from the feed line to the radiating patch, thereby minimizing reflection and improving impedance matching. In Antenna 2, a zeroth-order iteration of a modified fractal is etched onto the radiating patch. The introduction of the fractal geometry modifies the current distribution, effectively tuning the antenna to resonate at the desired frequency of 2.45 GHz. This geometry enables miniaturization while maintaining efficient radiation characteristics. Subsequently, Antenna 3 incorporates the first-order iteration of the fractal pattern. This iteration enhances the electrical length of the patch without increasing its physical dimensions, leading to an improved reflection coefficient and better impedance bandwidth. In Antenna 4, further optimization of the tapered feed line is performed to refine impedance matching and to suppress higher-order mode excitation. The modified feed line structure contributes to broader bandwidth and lower return loss, thereby improving antenna efficiency. Finally, Antenna 5 integrates higher-order fractal iterations along with a re-optimized tapered feed configuration. These enhancements result in the further reduction of the S_{11} parameter, increased

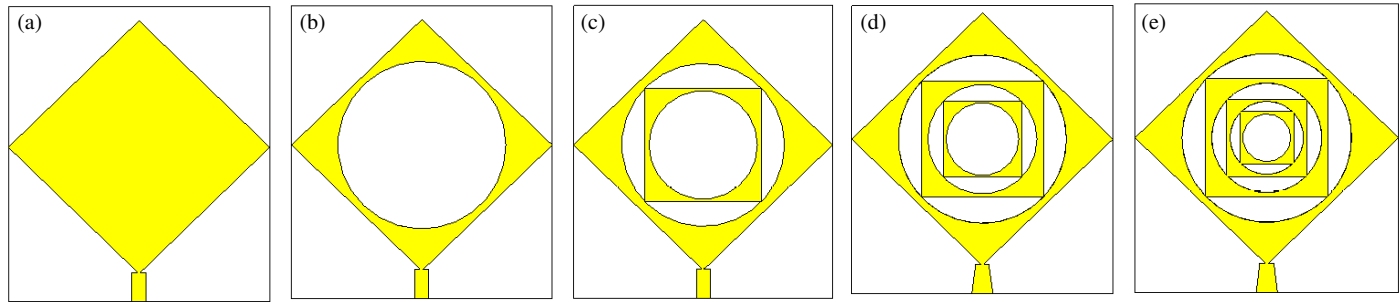


FIGURE 2. Step by step fractal iteration and design procedure of the proposed antenna. (a) Antenna 1 (without iteration), (b) Antenna 2 (Zeroth iteration), (c) Antenna 3 (First iteration), (d) Antenna 4 (Second iteration), (e) Antenna 5 (Third iteration).

bandwidth, and improved overall radiation characteristics, confirming the effectiveness of the fractal-based design approach for compact antenna applications.

Figure 3 shows the simulated reflection coefficient (S_{11}) for the antenna without iteration and with zeroth to third-order fractal iterations. The baseline antenna, without slots, shows limited performance. As the fractal iteration order increases, the resonant frequency shifts, and the reflection coefficient improves significantly. The third-order iteration achieves the best result, with $S_{11} = -60$ dB at 2.45 GHz, the target frequency for energy harvesting enhanced. This improvement is due to the altered surface current paths introduced by the fractal slot, which enhance impedance matching and bandwidth.

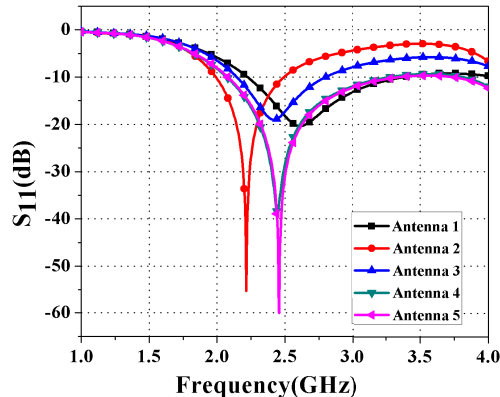


FIGURE 3. S_{11} (dB) variation of different antenna configurations.

3. SIMULATED PERFORMANCE OF THE PROPOSED ANTENNA

The surface current distributions of the proposed antenna at 2.45 GHz for different iterations are shown in Figures 4(a), (b), (c), (d), and (e). The surface current distribution becomes increasingly concentrated with higher fractal iterations. This is attributed to the increased electrical path length introduced by the fractal geometry without altering the physical size of the patch. At 2.45 GHz, the complex structure guides the current along well-defined paths near the feed point, resulting in high current density regions. These areas act as strong radiation sources, improving impedance matching and enhancing energy coupling into the resonant structure. This confirms that the pro-

posed fractal antenna efficiently operates at the single resonant frequency of 2.45 GHz.

4. VALIDATION OF THE PROPOSED ANTENNA

In order to verify the proposed antenna, a prototype is created as shown in Figures 5(a) and (b). The prototype was simulated by 3D EM simulation software HFSS (High-Frequency Structure Simulator). The S_{11} and gain performance of the prototype antenna are evaluated by Agilent N5247A vector network analyser and compared to the simulated performances, as illustrated in Figures 6(a) and (b).

The simulated and measured findings of S_{11} parameter correlate well, with a close match as shown in Figure 6(a). The return loss is satisfactory (-60 dB) at the resonance frequency (2.45 GHz), indicating that nearly all of the input power gets released with negligible reflection. Gain is a crucial parameter which is used to evaluate an antenna's qualities. The gain had a maximum value of 6.02 dBi and was measured in an omnidirectional direction. The antenna effectively radiates most of the input power, with a maximum radiation efficiency about 71.4%. The radiation efficiency of 71.4% indicates that approximately 28.6% of the input power is lost due to conductor and dielectric losses within the antenna structure. This efficiency value is mainly influenced by the loss tangent ($\tan \delta = 0.02$) of the FR-4 substrate used, as well as minor ohmic losses in the copper patch and ground plane. Although FR-4 is a low-cost material, its relatively high dielectric loss reduces efficiency compared to low-loss substrates such as Rogers RT/duroid. Nevertheless, the achieved efficiency of 71.4% is considered acceptable for ISM-band applications, where compactness and cost-effectiveness are prioritized over maximum efficiency.

Two-dimensional radiation patterns of the proposed antenna in the E -plane and H -plane at the target operating frequency are depicted in Figures 7(a) and 7(b), respectively. The copolarization characteristics exhibit a strong correlation between the simulated and measured results, thereby validating the accuracy of the antenna design and confirming the direction of maximum radiation. The cross-polarization levels are observed to be significantly low across both planes, indicating stable polarization performance. The antenna demonstrates a directional radiation pattern with enhanced gain in the intended direction, which is advantageous for ambient RF energy harvesting appli-

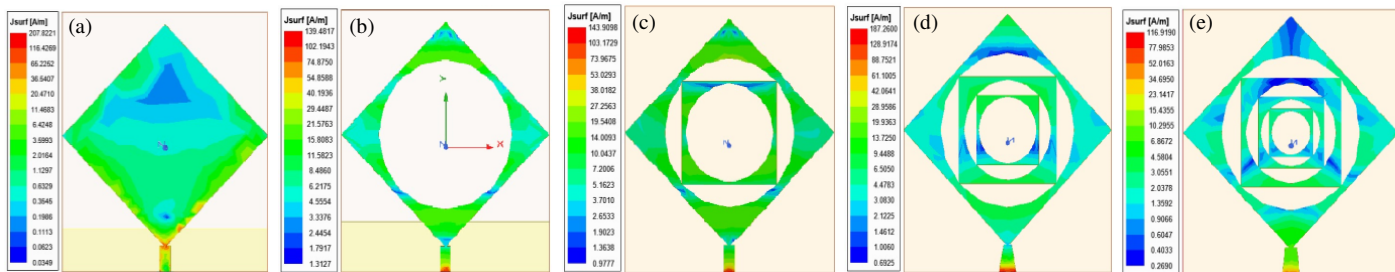


FIGURE 4. Surface current distribution of the proposed antenna at 2.45 GHz for different iterations. (a) Antenna 1 (without iteration), (b) Antenna 2 (Zeroth iteration), (c) Antenna 3 (First iteration), (d) Antenna 4 (Second iteration), (e) Antenna 5 (Third iteration).

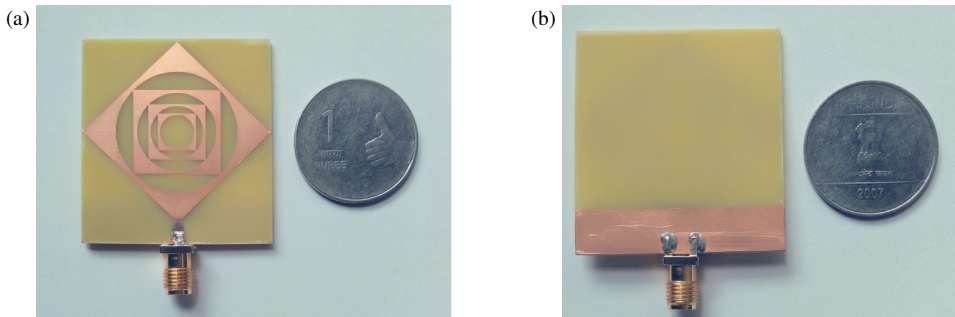


FIGURE 5. Fabricated prototype of the proposed antenna. (a) Front view. (b) Back view.

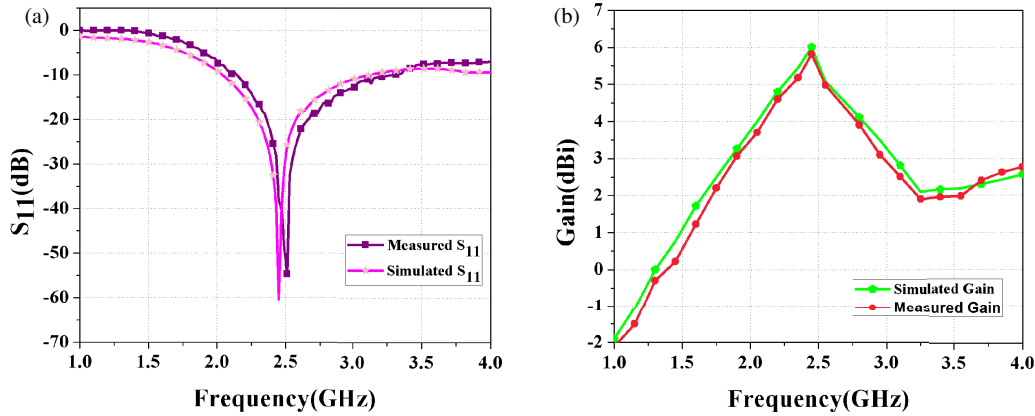


FIGURE 6. Simulated and measured parameters comparison. (a) S_{11} parameter. (b) Gain performance.

cations, as it facilitates efficient energy captured from specific directions.

Table 1 provides the comparison between the designed fractal antenna and existing designs by using the literature evolution. The proposed antenna outperforms existing designs in terms of return loss, gain, and bandwidth while maintaining a compact size. It achieves a return loss of -60 dB, gain of 6.02 dBi, and bandwidth of 1.23 GHz, which are better than antennas present in [18–21]. Thus, the design offers an excellent balance of compactness, wide bandwidth, and high performance for 2.45 GHz applications. One of the most important advantages of the proposed work is its low reflection coefficient (S_{11} parameter) and high gain which surpass the related values of the existing designs. The proposed antenna has compact size and easy structure while the existing literatures havw

larger and complex design structure than it. So it has also a great advantage regarding the cost and space.

5. PROPOSED RECTIFIER CIRCUIT CONFIGURATION

One of the most critical components in the design of a rectenna system is rectifier, which is responsible for converting ambient radio frequency (RF) energy into direct current (DC) power. The rectifier circuit is designed and simulated using Keysight Advanced Design System (ADS), a widely used tool for RF and microwave circuit design. The typical rectifier topology consists of a Schottky diode, load resistor, DC pass filter, and an impedance matching network (IMN). IMN plays a vital role in achieving impedance matching between the receiving antenna and the rectifier input, thereby ensuring maximum power trans-

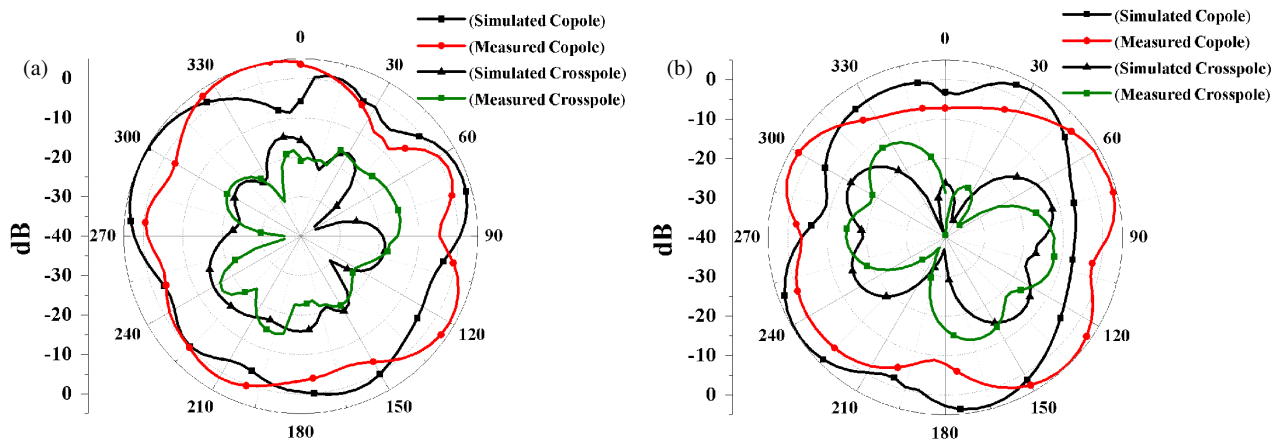


FIGURE 7. Simulated and measured co-pole and cross-pole radiation patterns at 2.45 GHz. (a) E plane. (b) H plane.

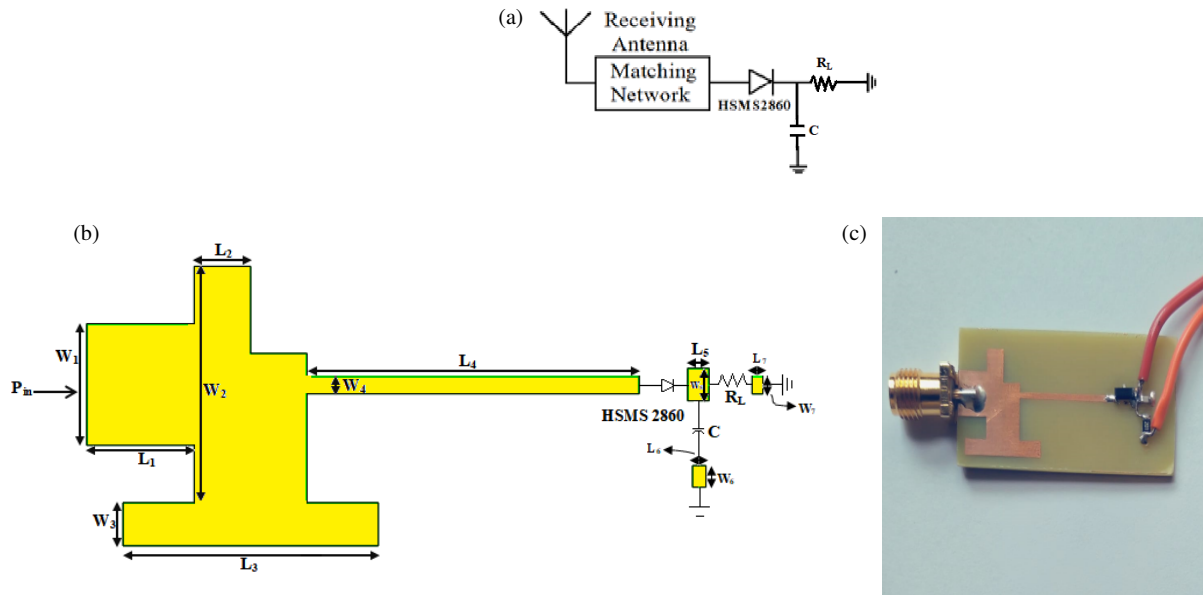


FIGURE 8. (a) Circuit diagram of the rectifier. (b) Schematic layout of the proposed rectifier circuit. (c) Fabricated prototype of the rectifier circuit.

fer at the target resonance frequency. Schottky diode is the most influential component in the rectifier circuit, as it predominantly dictates both the conversion efficiency and energy loss. Due to the inherently low power density of ambient RF sources, selecting a diode with low turn-on voltage and high switching speed is essential. Schottky diodes are preferred in such applications owing to these characteristics. Several diode families have been identified as suitable for RF energy harvesting, including HSMS-28XX series, SMS7630 series, and MA4E1317 series, each offering low barrier height and fast response times suitable for high-frequency, low-power scenarios. Here Schottky diode HSMS2860 is selected depending upon the available energy density [13]. Several rectifier structures, such as single diode [14, 15] and voltage doubler configurations [16, 17], were studied in order to produce DC voltage. Figure 8(a) illustrates the layout of the proposed single-band rectifier, which incorporates an impedance matching network (IMN) to ensure maximum power transfer between the antenna and rectifying circuit. The IMN is designed using microstrip transmission

lines with the following physical dimensions: $W_1 = 5.68$ mm, $L_1 = 5$ mm, $W_2 = 11$ mm, $L_2 = 2.93$ mm, $W_3 = 2$ mm, $L_3 = 11.8$ mm, $W_4 = 0.8$ mm, $L_4 = 15.6$ mm. The rectifier circuit includes a Schottky diode (HSMS-2860), a DC pass filter composed of a capacitor ($C = 47$ pF), and a load resistor ($R_L = 1250 \Omega$). The complete circuit is fabricated on an FR4 substrate with a dielectric constant of 4.3 and a thickness of 1.6 mm. Figure 8(a) shows the circuit model of the rectifier. Figure 8(b) displays the schematic layout of the proposed rectifier, and the fabricated prototype of the rectifier is shown in Figure 8(c), demonstrating a compact and practical implementation for RF energy harvesting applications.

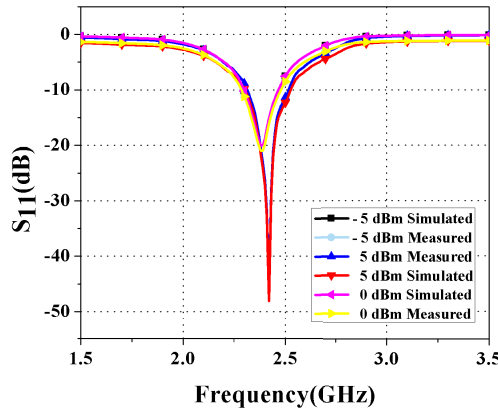
A parametric analysis was carried out to optimize the output voltage (V_{out}) and power conversion efficiency (PCE) of the proposed rectifier circuit. The simulated and measured results are presented in Figure 9, which displays the return loss (S_{11}) at three distinct input power levels: -5 dBm, 0 dBm, and 5 dBm, for a fixed load resistance of 1250Ω . The results indicate that variations in input power have a negligible effect on the res-

TABLE 1. Performance comparison of the fractal antenna with existing literatures.

References	Frequency (GHz)	Dimension (mm ³)	Return loss, S_{11} (dB)	BW (GHz)	Gain (dBi)
[18]	2.45	40 × 47.5 × 1.6	-52	0.15	3.48
[19]	2.45	48 × 48 × 1.6	-34	0.35	3.2
[20]	2.4	43 × 43 × 1.6	-30	0.20	5.6
[21]	2.45	60 × 50 × 1.6	-38	0.30	5.15
[25]	2.45	60 × 80 × 1.6	-48	1.38	3.62
This work	2.45	41.03 × 37.24 × 1.6	-60	1.23	6.02

TABLE 2. Performance comparison of the rectenna with existing literature.

References	Frequency (GHz)	Type of diode	Rectifier Topology	PCE (%)	P_{in} (dBm)	Load Resistance R_L (Ω)
[22]	2.4	SMS7630-005	VDR	65.1	0	4100
[23]	2.45	HSMS-286C	DGS Low-Pass Filter	63	18	-
[24]	2.45	SMS7630-079LF	Single stage voltage multiplier	62	2	3300
[25]	2.45	HSMS-2852	VDR	62.4	0	4000
This work	2.45	HSMS-2860	Single diode shunt rectifier	70.07	5	1250

**FIGURE 9.** Simulated and measured S_{11} vs. frequency of the proposed rectifier.

onance frequency and impedance matching performance, confirming that the rectifier operates in a linear and stable regime across the evaluated power levels. Consequently, the proposed rectifier demonstrates robust performance and maintains effective operation at the designed resonant frequency over a broad range of input power levels, which is desirable for practical ambient RF energy harvesting scenarios.

Figures 10(a) and (b) show the comparison of the Power Conversion Efficiency (PCE) and Output Voltage (V_{out}) as a function of Input Power (P_{in}) with matching network and without matching network for RF energy harvesting. The addition of a matching network (MN) significantly enhances V_{out} (DC output voltage of the rectifier) and PCE (Power Conversion Efficiency). The matching network plays an important role to maximize the PCE and DC output voltage by limiting the impedance mismatch and increasing the power transfer. This results in that

the rectifier can operate effectively at its operating frequency (2.45 GHz) for an input power ranging from -5 dBm to 5 dBm. The PCE and V_{out} are tested at 1250 Ω load resistance.

Figure 11(a) and 11(b) illustrate the impact of varying load resistance (R_L) on the performance of the RF energy harvesting system. The performance is evaluated in terms of Power Conversion Efficiency (PCE) and DC output voltage (V_{out}) as a functions of input power (P_{in}). As R_L increases from 800 Ω to 1250 Ω, the maximum PCE also increases, reaching a peak value of 70.07% at $P_{in} = 5$ dBm. At $P_{in} = 0$ dBm, the rectifier achieves a PCE of 59.96%. However, beyond a certain load resistance value (e.g., 1400 Ω), the PCE begins to decline, likely due to reduced current flow or suboptimal load matching conditions. The rectifier achieves a DC output voltage of 0.866 V at 0 dBm and 1.664 V at 5 dBm, demonstrating effective energy conversion over a practical power range. The proposed rectifier is designed using a minimal number of components to reduce cumulative losses and enhance overall system efficiency. The output DC voltage of the rectenna is primarily governed by the amount of RF power captured by the antenna and the rectifier's PCE, both of which directly influence the magnitude of V_{out} .

A comparative analysis with existing state-of-the-art rectifiers has been conducted to highlight the novelty and efficiency of the proposed rectenna. The comparison results are summarized in Table 2. The proposed rectifier, employing an HSMS-2860 Schottky diode, demonstrates notable power conversion efficiency (PCE) of 70.07% at an input power level of 5 dBm, making it the most efficient among the designs considered for comparison. In contrast, rectifiers based on other diode models exhibit lower PCEs at various input power levels. For instance, the rectifier using an HSMS-2852 diode achieves a maximum PCE of 62.4% at 0 dBm input power [25], while the SMS7630-

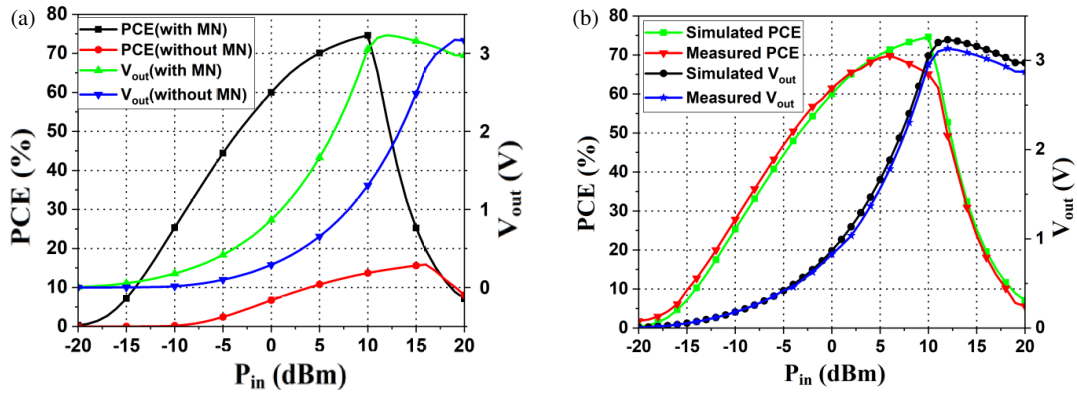


FIGURE 10. Performance variation of the proposed rectifier for PCE and V_{out} , (a) with and without Matching Network (MN), (b) simulated and measured results.

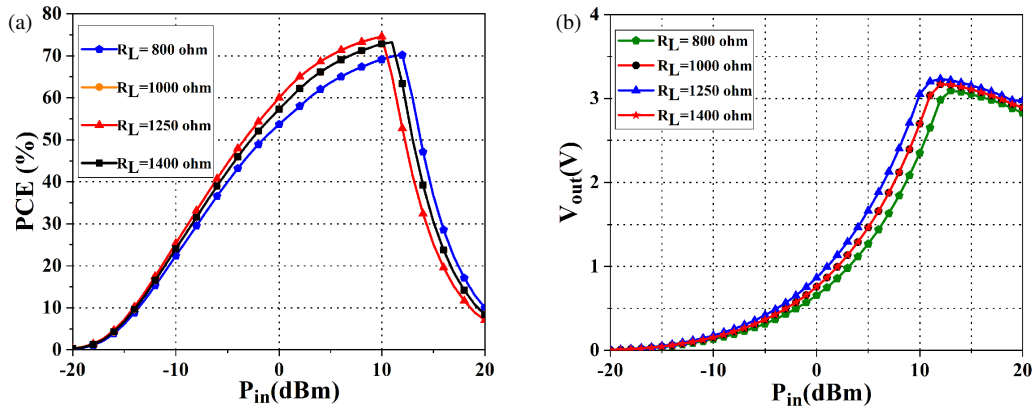


FIGURE 11. Simulated variation of the rectifier. (a) PCE vs. P_{in} , (b) V_{out} vs. P_{in} .

079LF diode reaches 62% at 2 dBm [24]. Similarly, the HSMS-286C diode yields a PCE of 63%, but only at a significantly higher input power level of 18 dBm [23]. The VDR-based rectifiers reported in [22] also demonstrate comparatively lower efficiency of 65.1%. These results confirm that the proposed rectifier exhibits superior performance and offers significant improvements in efficiency over existing designs, particularly under low-power ambient RF energy harvesting conditions.

6. EXPERIMENTAL VALIDATION OF THE RECTENNA SYSTEM

Figure 12(a) illustrates the experimental setup of a Radio frequency (RF) wireless power transmission system operating at 2.45 GHz, which falls within the Industrial, Scientific, and Medical (ISM) frequency band. The system is composed of two primary sections: transmitting section and receiving section. The transmitting section includes an RF signal generator and a horn antenna. The RF generator produces a continuous wave signal at 2.45 GHz, which serves as the source of RF energy. This energy is then radiated into free space by the horn antenna. The receiving section comprises a receiving antenna, a rectifying circuit (rectenna), and a digital multimeter. The receiving antenna captures the transmitted RF energy, which is then fed into the rectifier circuit. The rectifier converts the RF signal into DC output voltage, which is measured using the mul-

timeter. This measurement confirms the system's capability to harvest ambient RF energy and convert it into usable electrical power. The rectenna prototype is fabricated on an FR4 substrate and consists of a compact antenna connected to a rectifying circuit via an SMA connector, as shown in Figure 12(b). Due to infrastructure limitations, a standalone rectenna module is developed for measurement purposes. The rectenna is positioned at a maximum distance of 250 cm from the transmitting antenna, where the power density is approximately 0 dBm. Experimental results show that the proposed system achieves a peak Power Conversion Efficiency (PCE) of 69.28% at an input power level (P_{in}) of 5 dBm. The measured DC output voltage (V_{out}) is 0.54 V at 0 dBm and 1.451 V at 5 dBm, confirming the high efficiency and practical feasibility of the proposed rectenna for RF energy harvesting applications. The PCE was calculated using Equation (3).

$$\text{PCE} = \frac{V_{\text{out}}^2}{R_L \times P_{\text{in}}} \times 100(\%) \quad (3)$$

where,

PCE = Power Conversion Efficiency

V_{out} = DC output voltage (V)

R_L = Load Resistance (Ω)

P_{in} = Input Power

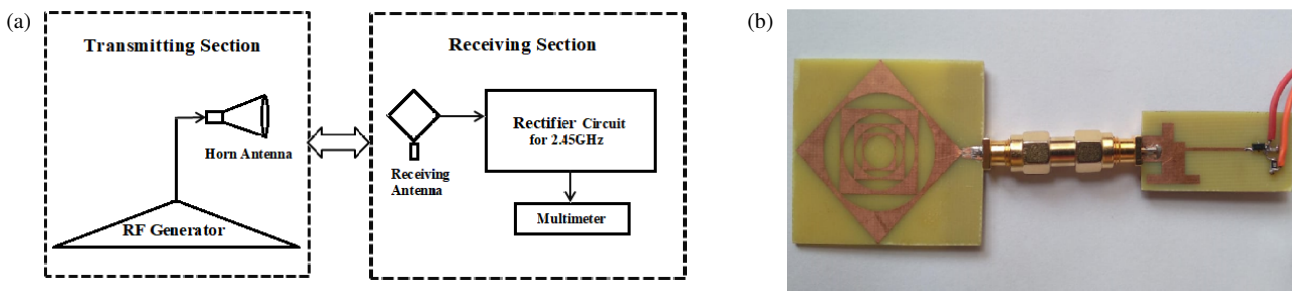


FIGURE 12. (a) Experimental setup of the rectenna. (b) Fabricated prototype of fractal-rectenna.

7. CONCLUSION

In this work, a single-band fractal antenna based on modified fractal carpet geometry has been designed and analyzed for efficient RF energy harvesting at 2.45 GHz. The antenna demonstrated excellent performance with a reflection coefficient of -60 dB, a wide bandwidth of 45.64% (ranging from 2.08 GHz to 3.31 GHz), a peak gain of 6.02 dBi, and a radiation efficiency of 71.4%. A rectifier circuit using an HSMS-2860 Schottky diode was successfully integrated with the antenna to form a rectenna system. The rectifier achieved a power conversion efficiency of 70.07% and produced a DC output voltage of 1.664 V under ambient RF conditions. The proposed rectenna is suitable for powering low-power electronic devices in wireless sensor networks (WSNs), Internet of Things (IoT) applications, and passive RF systems such as RFID and NFC. Its compact size, high efficiency, and ability to harvest ambient energy make it a viable solution for self-sustained wireless systems deployed in remote or hard-to-reach environments.

ACKNOWLEDGEMENT

We thankful to NIT Agartala for providing software support regarding simulation.

REFERENCES

- [1] Surender, D., M. A. Halimi, T. Khan, F. A. Talukdar, and Y. M. M. Antar, "A 90° twisted quarter-sectored compact and circularly polarized DR-rectenna for RF energy harvesting applications," *IEEE Antennas and Wireless Propagation Letters*, Vol. 21, No. 6, 1139–1143, 2022.
- [2] Shi, Y., J. Jing, Y. Fan, L. Yang, Y. Li, and M. Wang, "A novel compact broadband rectenna for ambient RF energy harvesting," *AEU — International Journal of Electronics and Communications*, Vol. 95, 264–270, 2018.
- [3] Haboubi, W., H. Takhedmit, J.-D. L. S. Luk, S.-E. Adami, B. Al-lard, F. Costa, C. Vollaire, O. Picon, and L. Cirio, "An efficient dual-circularly polarized rectenna for RF energy harvesting in the 2.45 GHz ISM band," *Progress In Electromagnetics Research*, Vol. 148, 31–39, 2014.
- [4] Shen, S., C.-Y. Chiu, and R. D. Murch, "A dual-port triple-band L-probe microstrip patch rectenna for ambient RF energy harvesting," *IEEE Antennas and Wireless Propagation Letters*, Vol. 16, 3071–3074, 2017.
- [5] Palazzi, V., M. Del Prete, and M. Fantuzzi, "Scavenging for energy: A rectenna design for wireless energy harvesting in UHF mobile telephony bands," *IEEE Microwave Magazine*, Vol. 18, No. 1, 91–99, 2017.
- [6] Liu, W., L. Xu, and H. Zhan, "Design of 2.4 GHz/5 GHz planar dual-band electrically small slot antenna based on impedance matching circuit," *AEU — International Journal of Electronics and Communications*, Vol. 83, 322–328, 2018.
- [7] Kuzu, S. and N. Akcam, "Array antenna using defected ground structure shaped with fractal form generated by Apollonius circle," *IEEE Antennas and Wireless Propagation Letters*, Vol. 16, 1020–1023, 2016.
- [8] Choukiker, Y. K., S. K. Sharma, and S. K. Behera, "Hybrid fractal shape planar monopole antenna covering multiband wireless communications with MIMO implementation for handheld mobile devices," *IEEE Transactions on Antennas and Propagation*, Vol. 62, No. 3, 1483–1488, 2014.
- [9] Mandelbrot, B. B., *The Fractal Geometry of Nature*, Freeman, San Francisco, CA, Jan. 1982.
- [10] Yadav, S., P. Jain, and R. Choudhary, "A novel approach of triangular-circular fractal antenna," in *International Conference on Advances in Computing, Communications and Informatics (ICACCI)*, 708–711, Delhi, India, 2014.
- [11] Singh, A. K., R. A. Kabeer, Z. Ali, and D. Gurjar, "Performance analysis of compact Koch fractal antennas at varying iterations," in *Students Conference on Engineering and Systems (SCES)*, 1–5, Allahabad, India, 2013.
- [12] Shrestha, S., S.-J. Han, S.-K. Noh, S. Kim, H.-B. Kim, and D.-Y. Choi, "Design of modified Sierpinski fractal based miniaturized patch antenna," in *The International Conference on Information Networking (ICOIN)*, 274–279, Bangkok, Thailand, 2013.
- [13] Surender, D., T. Khan, F. A. Talukdar, A. De, Y. M. M. Antar, and A. P. Freundorfer, "Key components of rectenna system: A comprehensive survey," *IETE Journal of Research*, Vol. 68, No. 5, 3379–3405, 2022.
- [14] Das, P., A. Karmakar, P. Halimi, M. A. and Bhowmik, and S. Huda, "A fractal-based single band DR-rectenna for RF energy harvesting," *Journal of Electromagnetic Waves and Applications*, Vol. 39, No. 8, 918–930, 2025.
- [15] Niotaki, K., A. Georgiadis, A. Collado, and J. S. Vardakas, "Dual-band resistance compression networks for improved rectifier performance," *IEEE Transactions on Microwave Theory and Techniques*, Vol. 62, No. 12, 3512–3521, 2014.
- [16] Contreras, A., B. Rodríguez, L. Steinfeld, J. Schandy, and M. Siniscalchi, "Design of a rectenna for energy harvesting on Wi-Fi at 2.45 GHz," in *Argentine Conference on Electronics (CAE)*, 63–68, Buenos Aires, Argentina, 2020.
- [17] Çelik, K. and E. Kurt, "A novel meander line integrated E-shaped rectenna for energy harvesting applications," *International Journal of RF and Microwave Computer-Aided Engineering*, Vol. 29,

No. 1, e21627, 2019.

[18] Assogba, O., A. K. Mbodji, S. Diagne, and A. K. Diallo, "Design of a rectenna in 2.45 GHz band frequency for energy harvesting," *Energy and Power Engineering*, Vol. 13, No. 9, 333–342, 2021.

[19] Shi, Y., Y. Fan, J. Jing, L. Yang, Y. Li, and M. Wang, "An efficient fractal rectenna for RF energy harvest at 2.45 GHz ISM band," *International Journal of RF and Microwave Computer-Aided Engineering*, Vol. 28, No. 9, e21424, 2018.

[20] Kuang, D., G. Dong, H. Nie, W. Xiong, and Y. Yang, "Novel double fractal patches structure Antenna-in-Package based on LTCC technology for 2.4 GHz applications," *International Journal of RF and Microwave Computer-Aided Engineering*, Vol. 28, No. 5, e21266, 2018.

[21] Surender, D., T. Khan, and F. A. Talukdar, "A low-profile single band dielectric resonator antenna for radio frequency energy harvesting," in *Advanced Communication Technologies and Signal Processing (ACTS)*, 1–5, Silchar, India, 2020.

[22] Surender, D., M. A. Halimi, T. Khan, F. A. Talukdar, S. K. Koul, and Y. M. M. Antar, "2.45 GHz Wi-Fi band operated circularly polarized rectenna for RF energy harvesting in smart city applications," *Journal of Electromagnetic Waves and Applications*, Vol. 36, No. 3, 407–423, 2022.

[23] Ji, S., H. Qi, and H. Zhang, "A novel rectenna for 2.45 GHz wireless power transmission with PBG antenna," in *CIE International Conference on Radar (RADAR)*, 1–3, Guangzhou, China, 2016.

[24] Chuma, E. L., L. de la Torre Rodríguez, Y. Iano, L. L. B. Roger, and M.-A. Sanchez-Soriano, "Compact rectenna based on a fractal geometry with a high conversion energy efficiency per area," *IET Microwaves, Antennas & Propagation*, Vol. 12, No. 2, 173–178, 2018.

[25] Dhar, A., P. Pattanayak, A. Kumar, D. S. Gurjar, and B. Kumar, "Design of a hexagonal slot rectenna for RF energy harvesting in Wi-Fi/WLAN applications," *International Journal of RF and Microwave Computer-Aided Engineering*, Vol. 32, No. 12, e23512, 2022.